

# NUMERICAL RESEARCH OF THE VISCOUS EFFECT OF THE BILGE KEEL ON THE DAMPING MOMENT

Rui Deng,

Wenyang Duan,

Shan Ma,

Yong Ma,

Shipbuilding Engineering College of Harbin Engineering University

Harbin, China

## ABSTRACT

*Bilge keels are effective passive devices in mitigating the rolling motion, and the usage of them covers almost all the sea going vessels. This paper focuses on the viscous effect of the bilge keel, ignored the effect of the free surface and the effect of the ship hull, for the general viscous characteristic of the bilge keel. In order to investigate the viscous effect of the bilge keel on the total damping moment, a special 2 dimensional numerical model, which includes a submerged cylinder with and without bilge keels, is designed for the simulation of forced rolling. Three important factors such as bilge keels width, rolling periods, as well as maximal rolling angles are taken into account, and the viscous flow field around the cylinder is simulated by some codes based on the viscous method in different conditions, in which the three factors are coupled. Verification and validation based on the ITTC method are performed for the cylinder without bilge keels in the conditions of different rolling periods and maximal rolling angles. The primary calculation of damping moment induced by the cylinder with 0mm, 4mm, and 10mm width bilge keels shows some interesting results, and a systematic analysis is conducted. The analysis of the damping moment components suggests there is phase difference between the damping moment induced by the cylinder and the bilge keels, and when the bilge keels width reaches a special size, the total damping moment is mitigated. The calculation of the damping moments induced by the cylinder with some larger bilge keels are also performed, and the results suggest that, the damping moment induced by the bilge keels is increased rapidly and becomes the dominant part in the total damping moment while the width of the bilge keels are increased, but the damping moment induced by the cylinder is not changed significantly. Some illustration of the vortices formation and shedding is included, which is the mechanism of the damping moment caused by the bilge keels. The present work shows an interesting problem, and it is useful for the bilge keel design.*

**Keywords:** calculation model, viscous code, phase difference, damping moment, bilge keel

## INTRODUCTION

Ships are susceptible to rolling motion especially subjected to beam sea, and the performance of seagoing surface vessels is affected by limiting the effectiveness of the crew, damaging cargo, and limiting the operation of on-board equipment. The rolling motion can be considered as linear motion while the maximal rolling angle is not large, and the problem can be analyzed by related theories. But, another motion defined as nonlinear motion which can not be investigated by the theories when the maximal rolling angle is quite large, is much more important and attracts the researchers since the damage it caused. Prediction of the nonlinear rolling motion is one of the most difficult things since it deals with a motion similar to a spring-mass damper system, poorly damped by ship generated waves, in addition to the action of waves from the seas. Compared with the other motions of the vessels, viscous effect contributes obviously in nonlinear rolling motion, and

the motion can not be calculated accurately by the traditional potential theory. Because of the complexity of the viscous flow, nonlinear rolling motion is researched mainly by model test and empirical formula for a long time. Parametric excitation for rolling motion is used in 1861 by Froude [6], and it is still under using by the researchers. Later, in 1977, Ikeda et al. [8] developed an empirical method to predict the roll damping according to a series of model experiments. Both these potential theories appeared weakly in the application until 1998, Yeung et al. [34] proposed a composite roll moment equation to address separately the wave damping and the viscous damping related to flow separations, and the viscous effect captured the attention of the researchers. In 2001, Chakrabarti [1] further decomposed the roll damping coefficient for a ship hull form to the skin friction of the hull, eddy shedding from the hull, free surface waves, lift effect damping, and bilge keel damping.

Meanwhile, some results of roll predictions in time domain based on potential flow [14][19] showed partially dependent on empirical roll damping data which was limited to the pertinence relation of frequency and ship form. In addition to the numerical calculation results, Kwang et al. [13] in 2004 measured the velocity field in the vicinity of the structure by particle image velocimetry (PIV), and elucidated that the viscous damping (also called the eddy making damping) in a vortical flow affected the rolling motion of a blunt body. For this reason, numerical methods are in urgent [33] need for simulations of viscous flow and larger amplitude motions of surface ships. An unsteady Reynolds-averaged Navier-Stokes method which is based on an extension of CFDShip-IOWA (a general-purpose code for computational ship hydrodynamics) was developed by Robert V. Wilson(2006) [21] to predict ship motions with larger amplitude and non-slender geometry, in comparison to traditional linearized methods. Since then, a new way to investigate the nonlinear rolling motion is implemented, in which viscous method takes an important part. LUO Min-li(2011) [15] simulated the single-degree-of-freedom forced motion of a ship section and computes added mass and damping coefficient of sway, heave, rolling and sway to roll mode Based on CFD RANS method. Pablo M. Carrica [18] simulated the fully appended ONR Tumblehome model DTMB 5613 with the ship hydrodynamics code CFDShip-Iowa v4.5 and validated against experiments of an auto-piloted, self propelled model ship. DTMB5512 model's roll damping motions at different initial roll angles were simulated based on CFD by YANG Bo [32], and vessel's roll damping coefficients are calculated through the simulation results. A RANS based CFD solver with VOF modeling of free surface was employed to investigate the forced rolling motion of an intact ship, sloshing of water in tank and forced rolling motion of a damage ship by Qiuxin Gao [20] in 2012. YANG Chun-lei [33] simulated free decay and forced rolling at various forward speeds and amplitudes for a 3-D ship hull and predicted ship roll damping, in which a RANS solver was employed and a dynamic mesh technique was adopted and discussed in detail. The latest contribution of the researchers shows that viscous effect is an important part in the prediction of the nonlinear rolling motion, and the numerical model which takes the viscous flow into account is fit for describing the motion.

Bilge keels, which are longitudinal appendages, are effective passive devices in mitigating the motion [24-27], and the application is extended to many types of vessels. H.H. Chun [7] (2001) investigated the roll damping characteristics of three models of a 3-ton class fishing vessel representing the bare hull and hull with bilge keels by the free roll decay tests in calm water and also in uniform head waves in a towing tank, suggested that the bilge keel contribute significantly to the increment of the roll damping for zero speed even for small fishing vessels. Latter, different methods were adopted to discover the damping mechanism. Multiple time scales was applied by M. Eissa [15] (2003) to construct a second-order uniform expansion of the non-linear rolling response of a ship in regular beam seas, and found that the damping moment consisted of the linear term associated with radiation and viscous damping and a cubic term due to frictional resistance

and eddies behind bilge keels and hard bilge corners. Kinnas et al. [11][12] used a finite volume based Navier–Stokes solver to study vertical flows around bilge keels, and pointed out that the primary damping mechanism arising from a bilge keel was the formation and shedding of vortices. Discrete vortex method was also an important method developed by Vaidhyanathan [29] and Yeung et al. [35]. And based on desingularized blob vortices, which is applicable to free surface flows in the roll damping calculation of vessels with bilge keels and showed similar results. Then, some researchers investigated the effect [4][17] of the bilge keels and the hydrodynamic force [2][5] of the vessels with bilge keels, including the hydrodynamic flow [3]. Generally, the design of bilge keel width for conventional vessels is a balance between appendage resistance and roll reduction, and the effect of the bilge keels width is rare discussed, except for some special conditions [22]. Only Krish P. Thiagarajan [28] performed an experimental study involving a range of bilge keel widths from 0% to 20% of half beam of a FPSO with rectangular geometry in 2010. Both free decay and forced oscillation tests were conducted on the range of geometries at different amplitudes and frequencies. The results were analyzed by potential method and the analysis shows that, for given amplitude of rolling motion, the damping coefficient increases with increasing bilge keel size up to a certain point and then declines. The influence of the surface wave induced by the geometry was included in the damping moment measured in the experiment, and the effect of the viscous flow was ignored by the potential method which was used to analyse the result, so it is necessary to take these two problems into account in order to present a clear relationship between the bilge keel width and the viscous damping moment. But an important question presented by Krish P. Thiagarajan is whether there is a point of diminishing marginal returns for damping due to a larger bilge keel. In this paper, examines of the effect of bilge keel size through numerical simulation are conducted involving a range of bilge keel widths from 0% to 10% of half beam of a cylinder, and the cylinder is submerged in the water. The calculation is performed based on the viscous theory, no surface wave is induced by the rolling motion, and the damping moments are analysed directly without any potential method. The results show that there is minimal damping moment for the geometry with bilge keels while the bilge keel gets a special width, and the total damping moment is increased while the bilge keel size is increased and larger than the special one.

## MATHEMATICAL MODEL

In order to avoid the influence of the surface wave induced by the motion of the geometry, a cylinder submerged in the water deep from the surface is used, and the model can be simplified as 2-D if the effect of the tip is ignored. In this way, the free surface is not necessary to simulate, also no need to take the buoyancy and gravity into account. The diameter of the two dimensional cylinder is defined as  $d$ , and the width of the bilge keel is defined as  $b$ . In the present paper, 1.0 m, the angle between bilge keels equals to  $\theta$  degrees, and  $\theta$  is variable in the different conditions. In the condition that cylinder without bilges, equals to 0, and the numerical model is shown in Fig.1.

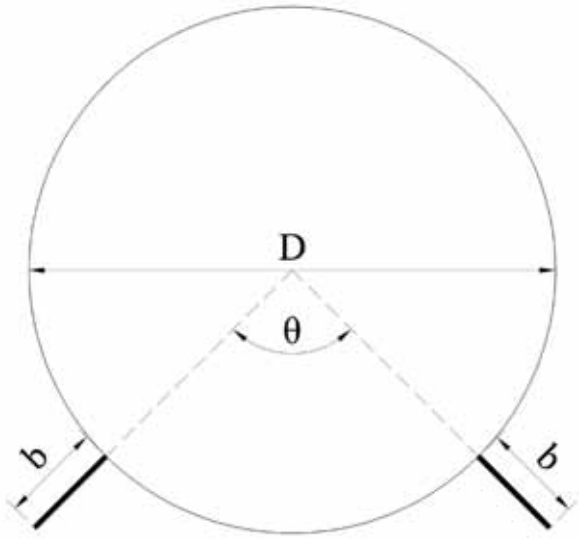


Fig. 1. Cylinder and the bilge keels

The rolling axis is the centre of the cylinder, and the function of the forced rolling motion is:

$$\varphi = \alpha \cos(\omega t + \alpha_0) \quad (1)$$

where  $\varphi$  is rolling angle,  $\alpha$  is the maximal rolling angle,  $\omega$  is rolling frequency,  $t$  is time, and  $\alpha_0$  is phase angle. The cylinder is defined at the equilibrium position which means  $\varphi = 0$  when  $t = 0$ , so  $\alpha_0$  is  $\pi/2$  in equation (1). The relationship between rolling frequency  $\omega$  and rolling period  $T$  is:

$$T = \frac{2\pi}{\omega} \quad (2)$$

Taken as incompressible viscous fluid, the flow field should satisfy the equations of continuity:

$$\frac{\partial u_i}{\partial x_i} = 0 \quad (i = 1, 2) \quad (3)$$

The unsteady incompressible RANS are:

$$\frac{\partial u_i}{\partial t} + \frac{\partial}{\partial x_j} (u_i u_j) = -\frac{\partial P}{\partial x_i} + \frac{\partial}{\partial x_j} \left( \mu \frac{\partial u_i}{\partial x_j} - \overline{u_i u_j} \right) \quad (4)$$

$(i, j = 1, 2)$

The turbulence model in the present simulations is the classical 2-equation eddy viscosity model,  $k-\omega$  Shear Stress Transport (SST) model, and the equations of which are presented as follows:

$$\frac{\partial k}{\partial t} + u_j \frac{\partial k}{\partial x_j} = \frac{\partial}{\partial x_j} \left[ \left( \nu + \frac{\nu_t}{\sigma_k} \right) \frac{\partial k}{\partial x_j} \right] + \nu_t \left[ \left( \frac{\partial \overline{u_i}}{\partial x_j} + \frac{\partial \overline{u_j}}{\partial x_i} \right) \frac{\partial \overline{u_i}}{\partial x_j} \right] - \beta^* f_{\beta} k \omega \quad (5)$$

$(i, j = 1, 2)$

$$\frac{\partial \omega}{\partial t} + u_j \frac{\partial \omega}{\partial x_j} = \frac{\partial}{\partial x_j} \left[ \left( \nu + \frac{\nu_t}{\sigma_\omega} \right) \frac{\partial \omega}{\partial x_j} \right] + \alpha \left[ \left( \frac{\partial \overline{u_i}}{\partial x_j} + \frac{\partial \overline{u_j}}{\partial x_i} \right) \frac{\partial \overline{u_i}}{\partial x_j} \right] - \beta \omega^2 + D_\omega \quad (6)$$

$(i, j = 1, 2)$

The calculation method of the parameters can be found in the related theories.

The equations are coupled through the Pressure Implicit Split Operator (PISO) algorithm. For spatial discretization, a second order up-wind difference scheme and a central difference scheme are applied. The damping force is obtained by the integration of the pressure on the cylinder and bilge keels. The damping moment of the cylinder is defined as the damping force times  $D/2$ , and the damping moment of the bilge keels is defined as an integral of the damping force along the bilge keels.

## VERIFICATION AND VALIDATION

For the simulation of the forced rolling motion of the 2-D cylinder under water with bilge keels, it is quite hard to perform experiment, but some mathematical methods can be used to verify and validate the calculation. The verification and validation (V&V) procedures, which is introduced and demonstrated by Wilson and Stern [23][30-31], and suggested by the ITTC [9][10] can be used to estimate the numerical and modelling errors along with uncertainties of the unsteady forced rolling motion simulations. Numerical uncertainty  $U_{SN}$  is decomposed into contributions from iteration number, grid size, time step, and other parameters. The uncertainties caused by iteration number, grid size, time step, and other parameters are defined as  $U_I$ ,  $U_G$ ,  $U_T$  and  $U_P$  respectively. Simulation error  $\delta_{SN}$  also can be caused by the factors above, and those simulation errors are defined as  $\delta_I$ ,  $\delta_G$ ,  $\delta_T$  and  $\delta_P$ . In the present work, the time step is fixed while discussing the grid errors, and the iterative errors are considered to be negligible in comparison to those due to grid, so the uncertainties  $U_{SN}$  and simulation errors  $\delta_{SN}$  are given by

$$U_{SN}^2 = U_I^2 + U_G^2 + U_T^2 + U_P^2 \approx U_G^2 \quad (6)$$

$$\delta_{SN} = \delta_I + \delta_G + \delta_T + \delta_P \approx \delta_G$$

Three groups of structural grids defined as Grid1, Grid2 and Grid3 are generated for the flow field with systematic refinement ratio  $r_G = \Delta x_{G1}/\Delta x_{G2} = \Delta x_{G2}/\Delta x_{G3}$  to estimate numerical errors and uncertainties due to grid size. The typically used refinement ratio  $r_G = \sqrt{2}$  is used in verification, and the grid spacing in the normal direction of the cylinder are 2.0 mm (coarse grid, Grid1) and 1.0 mm (fine grid, Grid3). Using of this refinement ratio also makes a great increase of grid amount, and the total quantity of coarse/medium/fine grids are about 35K/70K/140K correspondingly.

Three cases are investigated, and the forced rolling period  $T$  of each case is 2 seconds while the maximal roll angle  $\alpha$  are  $10^\circ$ ,  $20^\circ$  and  $30^\circ$  respectively. The solutions of the damping moments of the forced rolling motion in 10 periods with Grid1, Grid2, and Grid3 are  $S_1$ ,  $S_2$  and  $S_3$  and are shown in Fig.2, where the time coordinate of the damping moments history are rolling periods.

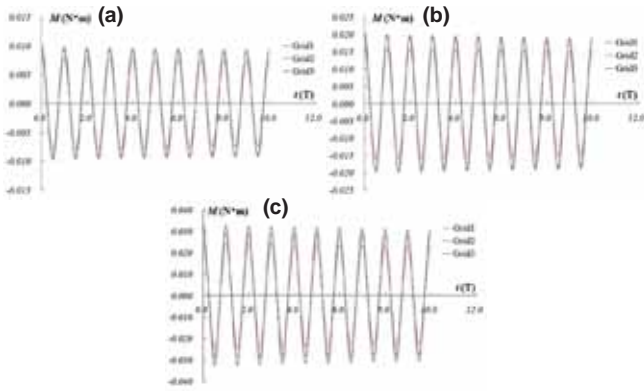


Fig. 2. Solution of each condition for (a) CASE1 ( $T=2.0s$ ,  $\alpha=10^\circ$ ) (b) CASE2 ( $T=2.0s$ ,  $\alpha=20^\circ$ ) and (c) CASE3 ( $T=2.0s$ ,  $\alpha=30^\circ$ )

Examination of solution changes between coarse/medium,  $\epsilon_{21} = S_2 - S_1$  and medium/fine,  $\epsilon_{32} = S_3 - S_2$  grids shows monotonic convergence  $\epsilon_{32} < \epsilon_{21}$  as shown in Fig.3. Where T indicates rolling period.

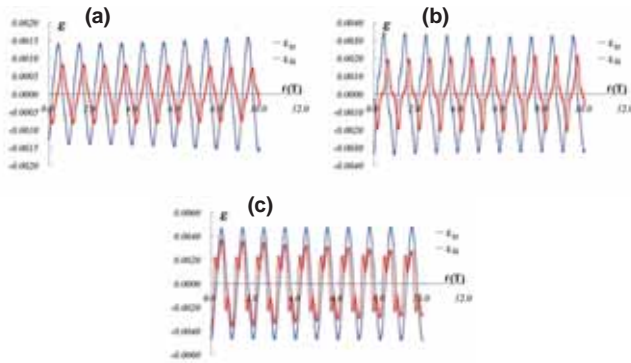


Fig. 3. Verification of predicted moment for 2-D cylinder of forced rolling for (a) CASE1( $T=2.0s$ ,  $\alpha=10^\circ$ ) (b) CASE2( $T=2.0s$ ,  $\alpha=20^\circ$ ) and (c) CASE3( $T=2.0s$ ,  $\alpha=30^\circ$ )

So that the convergence ratio  $R_G$  can be determined by

$$\langle R_G \rangle = \frac{\|\epsilon_{32}\|_2}{\|\epsilon_{21}\|_2} \quad (9)$$

and Richardson extrapolation (RE) can be used to estimate the order-of-accuracy  $p_G$ , and grid error  $\delta_{G1}$  of Grid1 by

$$\langle p_G \rangle = \frac{\ln(\|\epsilon_{21}\|_2 / \|\epsilon_{32}\|_2)}{\ln(r_G)} \quad (10)$$

$$\langle \delta_{G1} \rangle = \frac{\|\epsilon_{32}\|_2}{r_G^{\langle p_G \rangle - 1}} \quad (11)$$

where the correction factor  $C_G$  is given by

$$\langle C_G \rangle = \frac{r_G^{\langle p_G \rangle} - 1}{r_G^{\langle p_G \rangle_{est}} - 1} \quad (12)$$

where  $p_{G_{est}}$  is an estimate for the limiting order of accuracy as spacing size goes to zero and the asymptotic range is reached so that  $C_G \rightarrow 1$ . When solutions are far from the asymptotic

range,  $C_G$  is sufficiently less than or greater than 1 and only the magnitude of the error is estimated through the uncertainty  $U_G$ :

$$U_G = \left[ |C_G| + |1 - C_G| \right] \delta_{G1} \quad (13)$$

When  $C_G$  is less than 1, it can be estimated by

$$U_G = \left[ 2|1 - C_G| + 1 \right] \delta_{G1} \quad (14)$$

When solutions are close to the asymptotic range,  $C_G$  is close to 1 so that  $U_{GC}$  is estimated by

$$U_{GC} = \left| (1 - C_G) \delta_{G1} \right| \quad (15)$$

And the result is given in Table1.

Tab. 1. Verification of predicted damping moment for cylinder without bilge keels

| No.   | $P_G$ | $C_G$ | $\delta_{G1}$ | $U_G$ % |
|-------|-------|-------|---------------|---------|
| CASE1 | 2.02  | 1.02  | 0.02          | 2.25    |
| CASE2 | 1.87  | 0.91  | 0.05          | 0.06    |
| CASE3 | 1.15  | 0.49  | 0.20          | 0.39    |

From the convergence tests, it was found that solution  $S_3$  with the fine grid, Grid3, suffice for the convergence of the moment histories converged. The pressure gradient at the region around bilge keels varies significantly due to the presence of vortices, refining the grid size in the flow field will provide more accurate results. Therefore, Grid3 is used for the present simulation and the total number of elements is 140000.

## NUMERICAL RESULT AND ANALYSIS

In the primary research, the widths of the bilge keels are  $b = 0, 10$  and  $30$  mm ( $b = 0\%D$ ,  $b = 1\%D$  and  $b = 3\%D$ ), and  $b = 0$  mm means that no bilge keel is appended on the cylinder. The rolling periods are  $T = 2.0, 3.0$  and  $4.0$  s respectively, and the maximal rolling angle  $\alpha$  are  $10^\circ, 20^\circ$  and  $30^\circ$ . Calculations of the total damping moments of all the conditions in 10 rolling periods are performed and the results are shown in Fig 4, which has rolling periods as time coordinate.

Where T is the rolling period. An interesting thing is shown in Fig 4 that when the width of the bilge keel equals to 10 mm, the damping moments are less than the one of the cylinder without bilge keels. A problem arisen from the results is, the total damping moments of the cylinder with bilge keels which are of special size may be less than the those in the condition that without bilge keels. Analysis of the data suggests that the minimal damping moment can be obtained while the width of the bilge keel is about 4 mm. The damping moments of the cylinder without bilge keels and those of the cylinder with 4 mm width bilge keels are compared in Fig.5, and the damping moment history has rolling period as time coordinate. The rolling periods are  $T = 2.0, 3.0$  and  $4.0$  s, and the maximal rolling angle  $\alpha$  are  $10^\circ, 20^\circ$  and  $30^\circ$  respectively.

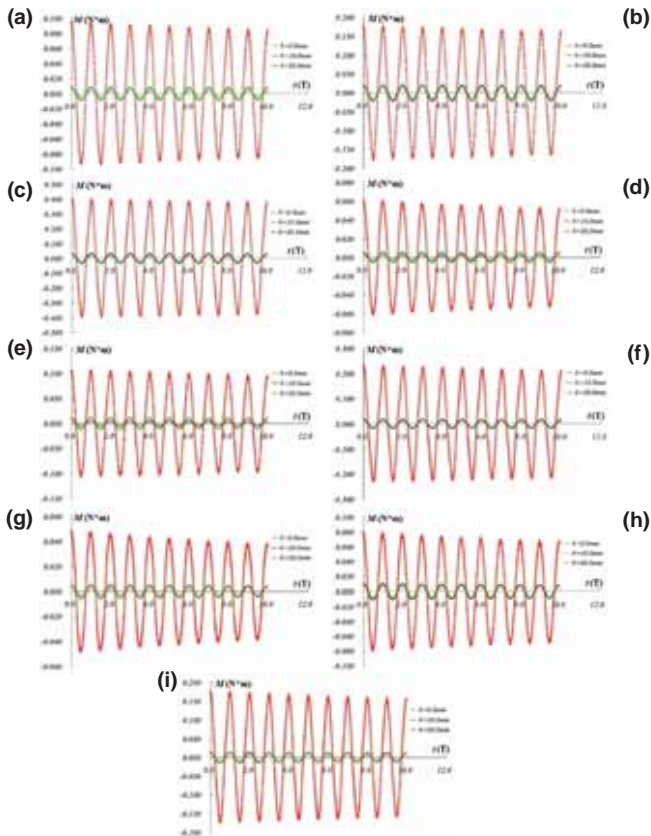


Fig. 4. Comparisons of the primary numerical results for (a)  $T=2.0s$ ,  $\alpha=10^\circ$ , (b)  $T=2.0s$ ,  $\alpha=20^\circ$ , (c)  $T=2.0s$ ,  $\alpha=30^\circ$ , (d)  $T=3.0s$ ,  $\alpha=10^\circ$ , (e)  $T=3.0s$ ,  $\alpha=20^\circ$ , (f)  $T=3.0s$ ,  $\alpha=30^\circ$ , (g)  $T=4.0s$ ,  $\alpha=10^\circ$ , (h)  $T=4.0s$ ,  $\alpha=20^\circ$  and (i)  $T=4.0s$ ,  $\alpha=30^\circ$

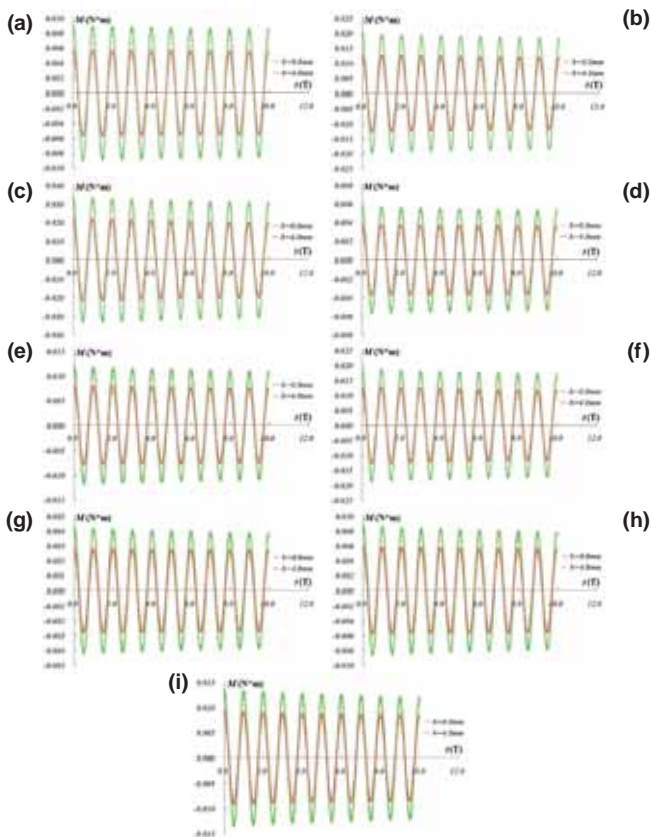


Fig. 5. Damping moment of the cylinder with bilge keels of given width for (a)  $T=2.0s$ ,  $\alpha=10^\circ$ , (b)  $T=2.0s$ ,  $\alpha=20^\circ$ , (c)  $T=2.0s$ ,  $\alpha=30^\circ$ , (d)  $T=3.0s$ ,  $\alpha=10^\circ$ , (e)  $T=3.0s$ ,  $\alpha=20^\circ$ , (f)  $T=3.0s$ ,  $\alpha=30^\circ$ , (g)  $T=4.0s$ ,  $\alpha=10^\circ$ , (h)  $T=4.0s$ ,  $\alpha=20^\circ$  and (i)  $T=4.0s$ ,  $\alpha=30^\circ$

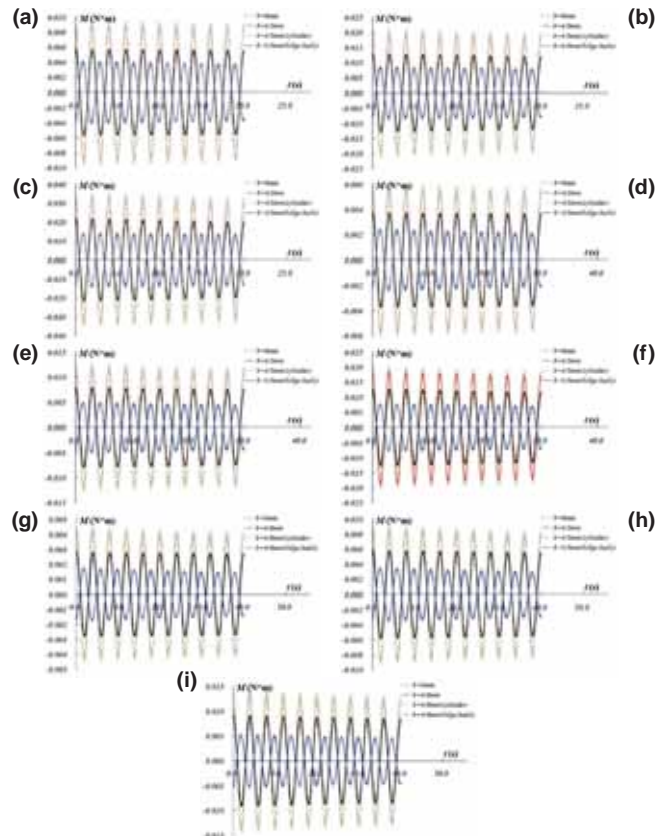


Fig. 6. Comparison of the damping moment composition for (a)  $T=2.0s$ ,  $\alpha=10^\circ$ , (b)  $T=2.0s$ ,  $\alpha=20^\circ$ , (c)  $T=2.0s$ ,  $\alpha=30^\circ$ , (d)  $T=3.0s$ ,  $\alpha=10^\circ$ , (e)  $T=3.0s$ ,  $\alpha=20^\circ$ , (f)  $T=3.0s$ ,  $\alpha=30^\circ$ , (g)  $T=4.0s$ ,  $\alpha=10^\circ$ , (h)  $T=4.0s$ ,  $\alpha=20^\circ$  and (i)  $T=4.0s$ ,  $\alpha=30^\circ$

Where the curve of  $b = 0$  mm indicates the damping moment history of cylinder without bilge keels, the curve of  $b = 4.0$  mm indicates the total damping moment history of cylinder with 4.0 mm width bilge keels, the curve of  $b = 4.0$  mm (cylinder) indicates the history of the damping moment induced only by the cylinder, and the curve of  $b = 4.0$  mm (bilge keels) indicates the history of the damping moment induced by bilge keels in the same condition. It is shown clearly in Fig.6 that the damping moment induced by the cylinder is not effected obviously whether the bilge keels are attached or not, but there is a phase difference between the damping moments induced by cylinder and the one induced by bilge keels. What is more, the magnitudes of these two damping moments are almost the same, so the total damping moments are reduced in the conditions that the 4 mm width bilge keels are attached. The result is interesting and useful for the design of the bilge keels.

It is shown in Fig.4 that if the width of the bilge keels is increased, the total damping moment increases also. In order to analyse the result carefully, two different cases which get the maximal and the minimum angular velocities are simulated, the rolling period is  $T = 2.0$  s and the maximal rolling angle  $\alpha$  is  $30^\circ$  for one case, and the rolling period is  $T = 4.0$  s and the maximal rolling angle  $\alpha$  is  $10^\circ$  for the other case. Comparison of the damping moments are performed in Fig.7, in which  $t$  is computation time.

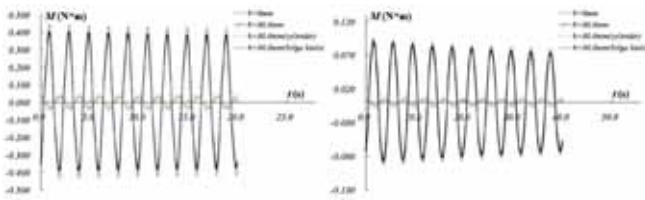


Fig.7. Comparison of the damping moment composition for (a)  $T=2.0s$ ,  $\alpha=30^\circ$ , (b)  $T=4.0s$ ,  $\alpha=10^\circ$

where the curve of  $b = 0$  mm indicates the damping moment history of cylinder without bilge keels, the curve of  $b = 30.0$  mm indicates the total damping moment history of cylinder with 30.0 mm width bilge keels, the curve of  $b = 30.0$  mm (cylinder) indicates the history of the damping moment induced only by the cylinder, and the curve of  $b = 30.0$  mm (bilge keels) indicates the history of the damping moment induced by bilge keels in the same condition. It can be seen from Fig.7 that the magnitudes of the damping moments induced by the cylinder are almost the same even the width of the bilge keels are 30.0 mm, but the damping moment induced by the bilge keels is increased obviously. There is still a phase difference between the damping moment induced by cylinder and the one induced by bilge keels, but the damping moment induced by the bilge keels is quite larger than the one induced by cylinder and becomes the dominant part of the total damping moment.

Some calculations about the total damping moment are performed, in which the bilge keel width is 50.0 mm, in order to investigate the influence of the bilge keel width on the damping moment. Comparisons of the total damping moments in 10 periods induced by cylinder without bilge keels, with 30.0 mm width bilge keels and 50.0 mm width bilge keels are performed in Fig.8, in which the damping moment history has computation time as time coordinate. The rolling periods are  $T = 2.0$  and  $4.0$  s respectively, and the maximal rolling angle  $\alpha$  are  $10^\circ$  and  $30^\circ$ .

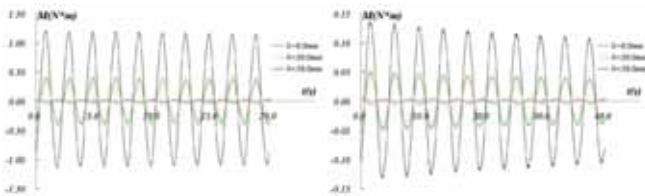


Fig.8. Comparison of the damping moments for (a)  $T=2.0s$ ,  $\alpha=30^\circ$ , (b)  $T=4.0s$ ,  $\alpha=10^\circ$

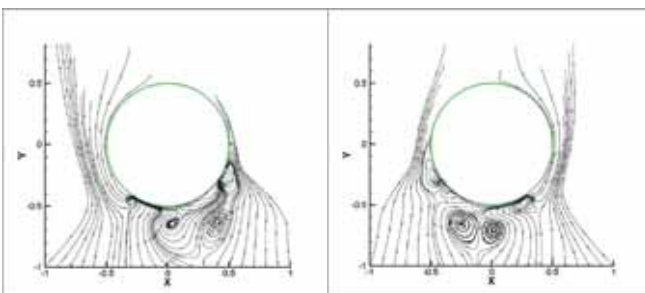


Fig. 9. Formation and shedding of vortices for (a)  $t = 1/4 T$ , (b)  $t = 3/4 T$

It is clearly shown in Fig.8 that when the cylinder is attached with 50.0 mm width bilge keels, the total damping moments induced by the cylinder and the bilge keels are larger than those induced by cylinder and 30.0 mm width bilge keels obviously, and they have the same trends which are different from those of the damping moments induced by the cylinder without bilge keels. It means that the damping moment induced by the bilge keels is increased rapidly while the width is increased, and it is the dominant part in the total damping moment.

The total damping moment induced by the cylinder with bilge keels in the present work is increased along with the increase of the bilge keel width when the width of the bilge keels is larger than the special size, and the primary damping mechanism arising from a bilge keel is the formation and shedding of vortices. The formation and shedding of vortices in a case is shown in Fig.9 in order to investigate the damping moment induced by bilge keels, in which the rolling period  $T$  is 4.0s, and the maximal rolling angle  $\alpha$  is  $30^\circ$ .

In Fig.9, it is shown that the flow field is affected by the bilge keels, and the vortices are formed around the bilge keels. Because of the rolling of the cylinder, the vortices are shedding from the bilge keels latter. After that, the vortices exist in the flow field for a long time and affect each other, for which the location and diameter of the vortices are affected. The formation and shedding of vortices are important reasons for the damping moment induced by the bilge keels, and Fig.9 shows an illustration for them. In the present work, the basic equation for the flow field is Reynolds Average Navier-Stokes equation, so the averaged velocity is used in the calculation and some of the small vortices are ignored.

## CONCLUSION

In order to investigate the effect of bilge keels on the damping moment, a special two dimensional model is designed and studied. In this way, some factors such as the influence of the surface wave, the interaction between the cylinder and the induced wave, as well as the effect of the length of the bilge keels are ignored. A viscous code based on the SST  $k - \omega$  viscous model is developed and used for the simulation of the forced rolling motion; the results are verified and validated by suggested method. An interesting issue shown in the results is that there is a phase difference between the damping moment induced by the cylinder and bilge keels, so the total damping is mitigated when the bilge keel width gets a special size. If the width of the bilge keel is increased and larger than the special size, the damping moment induced by the cylinder is not changed obviously, which means the flow field around the cylinder is affected by the bilge keel size weakly. But the damping moment induced by the bilge keels is increased quickly, and become the dominant part in the total damping moment. The formation and shedding of vortices is shown in detail. The numerical model used in the paper seems significant for the investigation of the bilge keels' effect. The viscous method is well known, but the usage of it for the analysis of the damping moment components and the relationship seems to be new and turns out to be useful for the design of the bilge keel.

## ACKNOWLEDGEMENTS

The support has been provided by the Fluid Mechanics Group led by DUAN Wen-yang of Harbin Engineering University. These Financial support has been provided by the National Natural Science Foundation of China (Grant No. 51209048; 51309069; 51379045); Research on Analysis and Forecasting Technology of Trimaran Hydrodynamic Performance; Research on the Distribution of Ship Energy Consumption and Energy Efficiency; National Defense Basic Research Foundation of China (Grant No. B2420132001); Fundamental Research Funds for the Central Universities (Grant No. HEUCF140101; P013513013)

## REFERENCES

1. Chakrabarti, S. Empirical calculation of roll damping of ships and barges, *Ocean Engineering*, Vol. 28, pp. 915-932, 2001.
2. Cueva, M, Hansen, AS, Silva, JLB, Faria, F, Morato, A. HYDRODYNAMICS OF AN INSTALLATION BARGE WITH BILGE KEELS AND STINGER, 29th ASME International Conference on Ocean, Offshore and Arctic Engineering, Shanghai, PEOPLES R CHINA, JUN 06-11, 2010.
3. D. Mylonas, P. Sayer. The hydrodynamic flow around a yacht keel based on LES and DES, *Ocean Engineering*, Vol. 46, pp. 18-32, 2012.
4. Dai, CM, Miller, RW, Percival, AS. HYDRODYNAMIC EFFECTS OF BILGE KEELS ON THE HULL FLOW DURING STEADY TURNS, *OMAE*, Vol. 5, pp. 571-580, 2009.
5. E.P. Bangun, C.M. Wang, T. Utsunomiya. Hydrodynamic forces on a rolling barge with bilge keels, *Applied Ocean Research*, Vol. 32, pp. 219-232, 2010.
6. Froude, W. On the Rolling of Ships, Ph.D. thesis, Royal Institute of Naval Architects, 1861.
7. H.H. Chun, S.H. Chun, S.Y. Kim. Roll damping characteristics of a small fishing vessel with a central wing, *Ocean Engineering*, Vol. 28, pp. 1601-1619, 2001.
8. IKEDA Y., HIMENO Y, TANAKA N. On eddy making component of roll damping force on naked hull, *Journal of the Society of Naval Architects of Japan*, Vol. 142, pp. 54-64, 1977.
9. ITTC QM Procedure (2002). 7.5- 03- 01- 01.
10. ITTC QM Procedure (2002). 7.5- 03- 02- 01.
11. Kinnas, S. A., Yu, Y. H., Kacham, B., Lee, H. A Model of the Flow Around Bilge Keels of FPSO Hull Sections Subject to Roll Motions, *Proceedings of the 12th Offshore Symposium, Soc. Naval Arch. Mar. Engr.. Houston TX., 2003.*
12. Kinnas, S. A. FPSO Roll Motions, Technical Report, Minerals Mgt. Service, USA, 2005.
13. Kwang Hyo Jung, Kuang-An Chang, Erick T. Huang. Two-dimensional flow characteristics of wave interactions with a free-rolling rectangular structure, *Ocean Engineering*, Vol. 32, pp. 1-20, 2005.
14. LI Yi-le, LIU Ying-zhong, MIAO Guo-ping. Potential flow solution using higher order boundary element method with Rankine source, *Journal of Hydrodynamics(Ser. A)*, Vol. 14, no 1, pp. 80-89, 1999.
15. LUO Min-li, MAO Xiao-fei, WANG Xiao-xia. CFD based hydrodynamic coefficients calculation to forced motion of two-dimensional section, *CHINESE JOURNAL OF HYDRODYNAMICS*, Vol. 26, no. 4, pp. 509-515, 2011.
16. M. Eissa, A.F. El-Bassiouny. Analytical and numerical solutions of a non-linear ship rolling motion, *Applied Mathematics and Computation*, Vol. 134, pp. 243-270, 2003.
17. Maimun, A. Priyanto, K.S. Wong, M. Pauzi, M. Rafiqul. Effects of side keels on patrol vessel safety in astern waves, *Ocean Engineering* 2009; 36: 277-284.
18. Pablo M. Carrica, Hamid Sadat-Hosseini, Frederick Stern. CFD analysis of broaching for a model surface combatant with explicit simulation of moving rudders and rotating propellers, *Computers & Fluids*, Vol. 53, pp. 117-132, 2012.
19. PU Jin-yun, ZHANG Wei-kang, JIN Tao. Melnikov's method for non-linear rolling motions of a flooded ship, *Journal of Hydrodynamics(Ser. B)*, Vol. 17, no. 5, pp. 580-584, 2005.
20. Qiuxin Gao, Dracos Vassalos. Numerical study of damage ship hydrodynamics, *Ocean Engineering*, Vol. 55, pp. 199-205, 2012.
21. Robert V. Wilson, Pablo M. Carrica, Fred Stern. Unsteady RANS method for ship motions with application to roll for a surface combatant, *Computers & Fluids*, Vol. 35, pp. 501-524, 2006.
22. Souza Jr., J.R., Fernandes, A.C., Masetti, I.Q., da Silva, S., Kroff, S.A.B.. Nonlinear rolling of an FPSO with larger-than-usual bilge keels, *Proceedings of the International Conference on Offshore Mechanics and Arctic Engineering – OMAE*, Lisbon, Portugal; July 5, 1998 - July 9, 1998.
23. Stern F, Wilson R, Coleman H, Paterson E. Comprehensive approach to verification and validation of CFD simulations—Part 1: Methodology and procedures, *ASME J Fluids Eng.*, Vol. 123, pp. 793-802, 2001.

24. Tanaka, N., Hishida, T. A Study on the Bilge Keels. Part 1. Two Dimensional Model Experiments, *J. Soc. Nav. Archit. Jpn.*, Vol. 101, pp. 99-105, 1957.
25. Tanaka, N. A Study on the Bilge Keels. Part 2. Full Sized Model Experiment, *J. Soc. Nav. Archit. Jpn.*, Vol. 103, pp. 69-73, 1958.
26. Tanaka, N. A Study on the Bilge Keels. Part 3. The Effect of the Ship Form and the Bilge Keel Size on the Action of the Bilge Keel, *J. Soc. Nav. Archit. Jpn.*, Vol. 105, pp. 27-32, 1959.
27. Tanaka, N. A Study on the Bilge Keels. Part 4. On the Eddy making Resistance to the Rolling of a Ship Hull, *J. Soc. Nav. Archit. Jpn.*, Vol. 109, pp. 205-212, 1960.
28. Thiagarajan, Krish P., Braddock, Ellen C. Influence of Bilge Keel Width on the Roll Damping of FPSO, 24th International Conference on Offshore Mechanics and Arctic Engineering, Halkidiki, GREECE; JUN 12-17, 2005.
29. Vaidhyathan, M. Separated Flows Near a Free Surface. Ph.D. thesis, University of California, Berkeley, CA., 1993.
30. Wilson R, Stern F, Coleman H, Paterson E. Comprehensive approach to verification and validation of CFD simulations—Part 2: Application for RANS simulation of a cargo/container ship, *ASME J Fluids Eng.*, Vol. 123, pp. 803-810, 2001.
31. Wilson R, Shao J, Stern F. Discussion: Criticisms of the correction factor verification method, *ASME J Fluids Eng.*, Vol. 125, pp. 732-733, 2003.
32. YANG Bo, WANG Zuo-chao, WU Ming. Numerical Simulation of Naval Ship's Roll Damping Based on CFD, *Procedia Engineering*, Vol. 37, pp. 14-18, 2012.
33. YANG Chun-lei, ZHU Ren-chuan, MIAO Guo-ping, FAN Ju. Numerical simulation of rolling for 3-D ship with forward speed and nonlinear damping analysis, *Journal of Hydrodynamics(Ser. B)*, Vol. 25, no. 1, pp. 148-155, 2013.
34. Yeung, R.W., Liao, S.-W., Roddier, D. Hydrodynamic coefficients of rolling rectangular cylinders, *Eighth International Journal of Offshore and Polar Engineers*, Vol. 8, pp. 242-250, 1998.
35. Yeung, R., Roddier, D., Alessandrini, B., Gentaz, L., and Liao, S.-W. On Roll Hydrodynamics of Cylinders Fitted With Bilge Keels, *Proceedings 23rd Symposium Naval Hydrodynamics*, Washington, DC., 2000.

## CONTACT WITH AUTHOR

Rui Deng  
e-mail: dengrui@hrbeu.edu.cn

Wenyang Duan

Shan Ma

Yong Ma

Shipbuilding Engineering  
College of Harbin Engineering University  
No.145 Nantong street  
150001 Harbin  
China

Tel.: +86-0451-8251-9901

fax: +86-0451-8251-9910